



Titre: In situ brain tumor detection using a Raman spectroscopy system —
Title: results of a multicenter study. Supplément

Auteurs: Katherine Ember, Frédérick Dallaire, Arthur Plante, Guillaume
Authors: Sheehy, Marie-Christine Guiot, Rajeev Agarwal, Rajeev Yadav, Alice
Douet, Juliette Selb, Jean Philippe Tremblay, Alex Dupuis, Eric
Marple, Kirk Urmev, Caroline Rizea, Armand Harb, Lily McCarthy,
Alexander Schupper, Melissa Umphlett, Nadejda Tsankova, Frédéric
Leblond, Constantinos Hadjipanayis, & Kevin Petrecca

Date: 2024

Type: Article de revue / Article

Référence: Ember, K., Dallaire, F., Plante, A., Sheehy, G., Guiot, M.-C., Agarwal, R., Yadav, R.,
Citation: Douet, A., Selb, J., Tremblay, J. P., Dupuis, A., Marple, E., Urmev, K., Rizea, C.,
Harb, A., McCarthy, L., Schupper, A., Umphlett, M., Tsankova, N., ... Petrecca, K.
(2024). In situ brain tumor detection using a Raman spectroscopy system —
results of a multicenter study. Scientific Reports, 14, 14 (12 pages).
<https://doi.org/10.1038/s41598-024-62543-9>

 **Document en libre accès dans PolyPublie**
Open Access document in PolyPublie

URL de PolyPublie: <https://publications.polymtl.ca/58635/>
PolyPublie URL:

Version: Matériel supplémentaire / Supplementary material
Révisé par les pairs / Refereed

Conditions d'utilisation: CC BY
Terms of Use:

 **Document publié chez l'éditeur officiel**
Document issued by the official publisher

Titre de la revue: Scientific Reports (vol. 14)
Journal Title:

Maison d'édition: Springer Nature
Publisher:

URL officiel: <https://doi.org/10.1038/s41598-024-62543-9>
Official URL:

Mention légale: This article is licensed under a Creative Commons Attribution 4.0 International License,
Legal notice: which permits use, sharing, adaptation, distribution and reproduction in any medium or
format, as long as you give appropriate credit to the original author(s) and the source,
provide a link to the Creative Commons licence, and indicate if changes were made. The
images or other third party material in this article are included in the article's Creative
Commons licence, unless indicated otherwise in a credit line to the material. If material

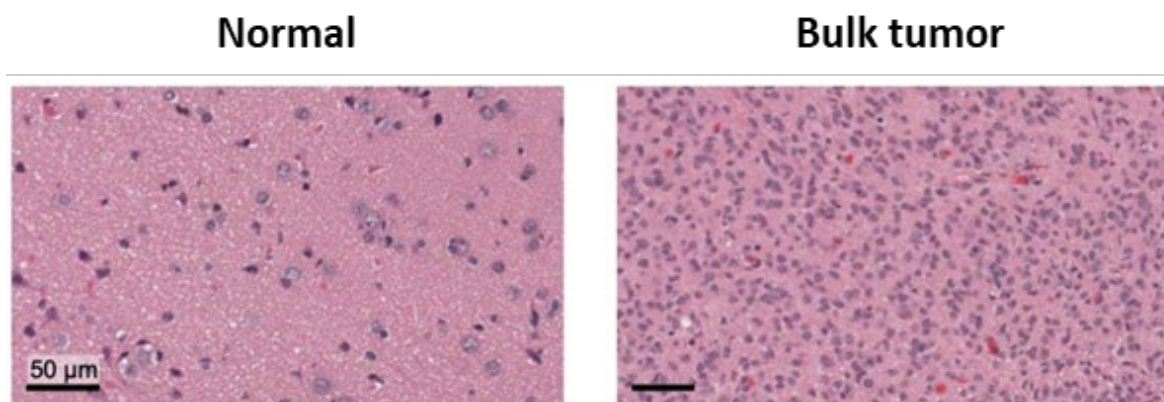


is not included in the article's Creative Commons licence and your intended use is not permitted by statutory regulation or exceeds the permitted use, you will need to obtain permission directly from the copyright holder. To view a copy of this licence, visit <http://creativecommons.org/licenses/by/4.0/>.

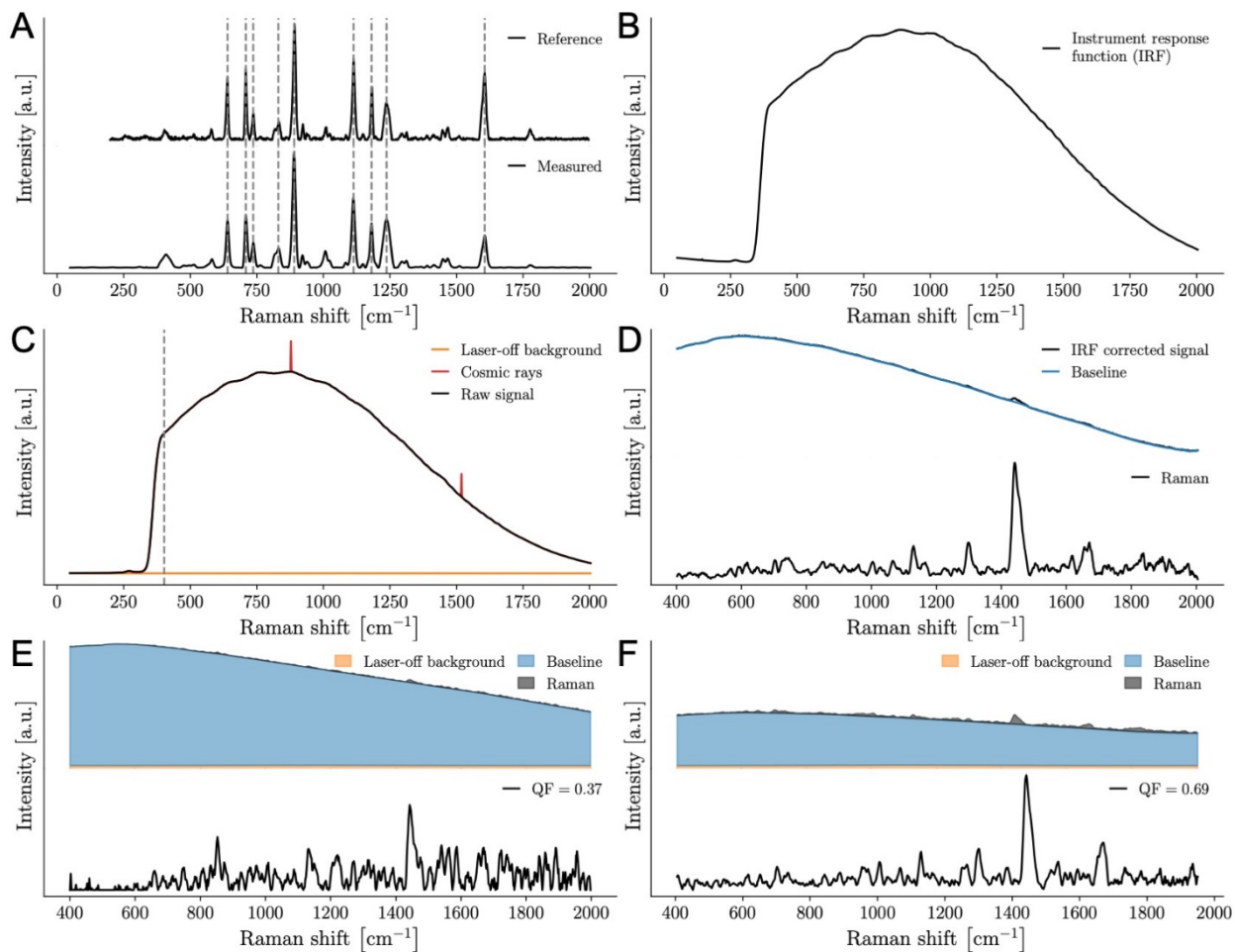
Supplementary figures and tables

Table S1. Assignment of Raman-active biomolecular vibrational modes from literature. The features (peak center) assigned to “lipid” are in comparison to spectral fingerprints from purified brain lipids⁴⁵ including phosphatidylethanolamine, phosphatidylcholine and sphingomyelin.²⁸ The features assigned to “protein” are in comparison to spectral fingerprints from purified proteins such as collagen.²⁶ Legend: C-H: carbon-hydrogen single bonds, C=C: carbon-carbon double bonds (unsaturated), C-C: carbon-carbon bonds, CH₂: ethyl group, CH₃: methyl group.

Spectral feature (peak center)	Biomolecular assignment
831 cm ⁻¹	Protein (tyrosine) ^{10,12}
856 cm ⁻¹	Protein (tyrosine) ^{10,12}
1004 cm ⁻¹	Protein (phenylalanine) ^{10,12}
1086 cm ⁻¹	Lipid (C–C bonds), ¹³ phosphate (phospholipids, nucleic acids) ^{13,14}
1131 cm ⁻¹	Lipid (C–C bonds) ¹³
1250–1260	Protein (amide), ¹⁰ lipid (unsaturated)
1299 cm ⁻¹	Lipid (saturated bonds, CH ₂) ¹³
1340 cm ⁻¹	Protein (tryptophan, C–H) ^{10,12}
1441 cm ⁻¹	Lipid (saturated bonds, CH ₂ , CH ₃), ¹³ protein (C–H) ¹⁰
1550 cm ⁻¹	Protein (tryptophan) ^{10,12}
1621 cm ⁻¹	Protein (tyrosine, tryptophan, phenylalanine) ^{10,12}
1659 cm ⁻¹	Lipid (unsaturated C=C), ¹³ protein (amide) ¹⁰



Supplementary Figure S1: Haematoxylin and eosin stains of normal and bulk tumor brain tissue sections. “Normal brain” indicates a cancer burden of 0% and whilst a cancer burden of >90% is “tumor” tissue. The scale bar is 50 micrometers. This example is from a patient with glioblastoma.



Supplementary Figure S2: (A-F) Data processing process. (A) Reference spectrum of polycarbonate used to convert CCD camera pixels into wavenumbers based on a polycarbonate spectrum measured with the Sentry system. (B) Instrument response function (IRF) measured with the system from the National Institute of Standards and Technology (NIST) Raman standard. (C) Dark count background acquired with the laser turned off and unprocessed (raw) *in situ* brain spectrum showing cosmic ray events. The grey dotted line designates the region that is truncated before further spectral pre-processing. (D) Spectrum after removal of cosmic rays and normalization with the IRF with the non-Raman baseline contribution isolated using the BubbleFiill shown in blue. The SNV-normalized Raman spectrum is shown at the bottom. (E-F) Representation of correction applied to (E) one low quality spectrum (QF = 0.37) and (F) one high quality spectrum (QF = 0.69).

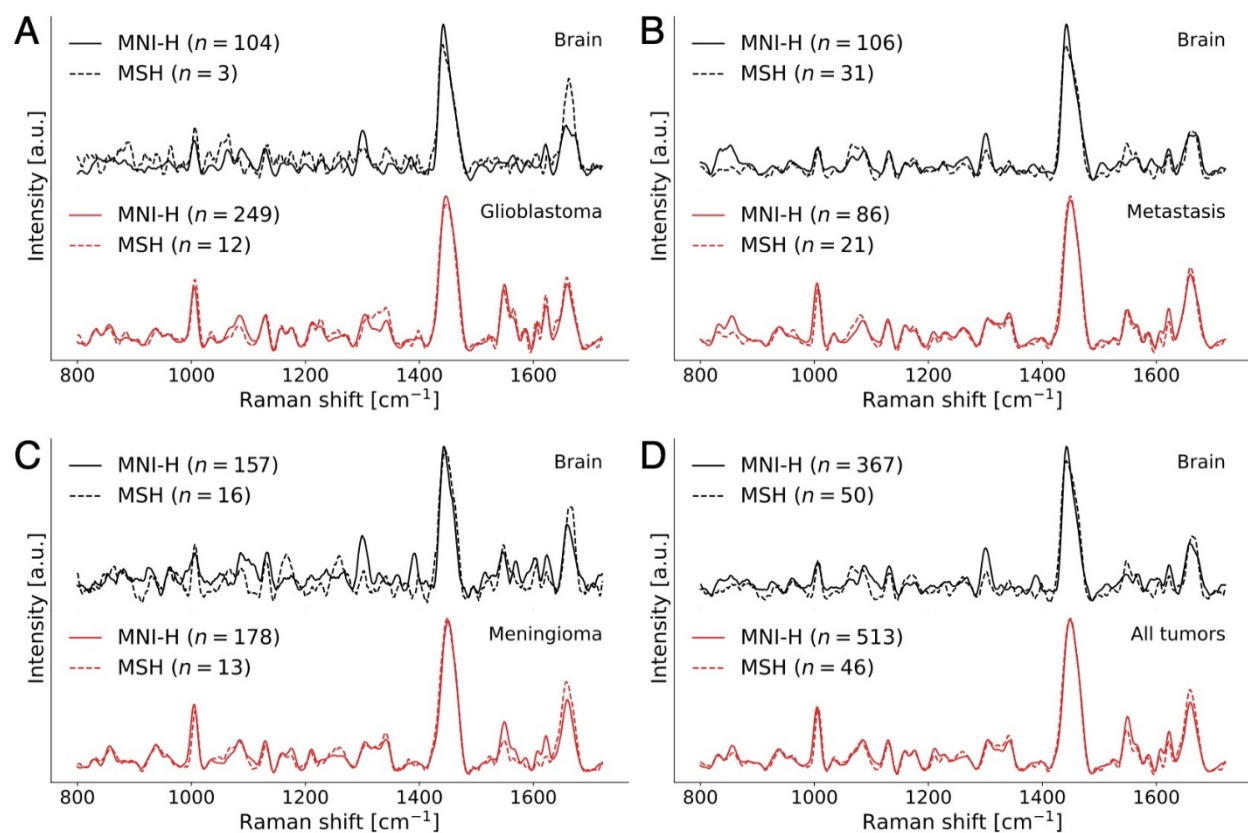
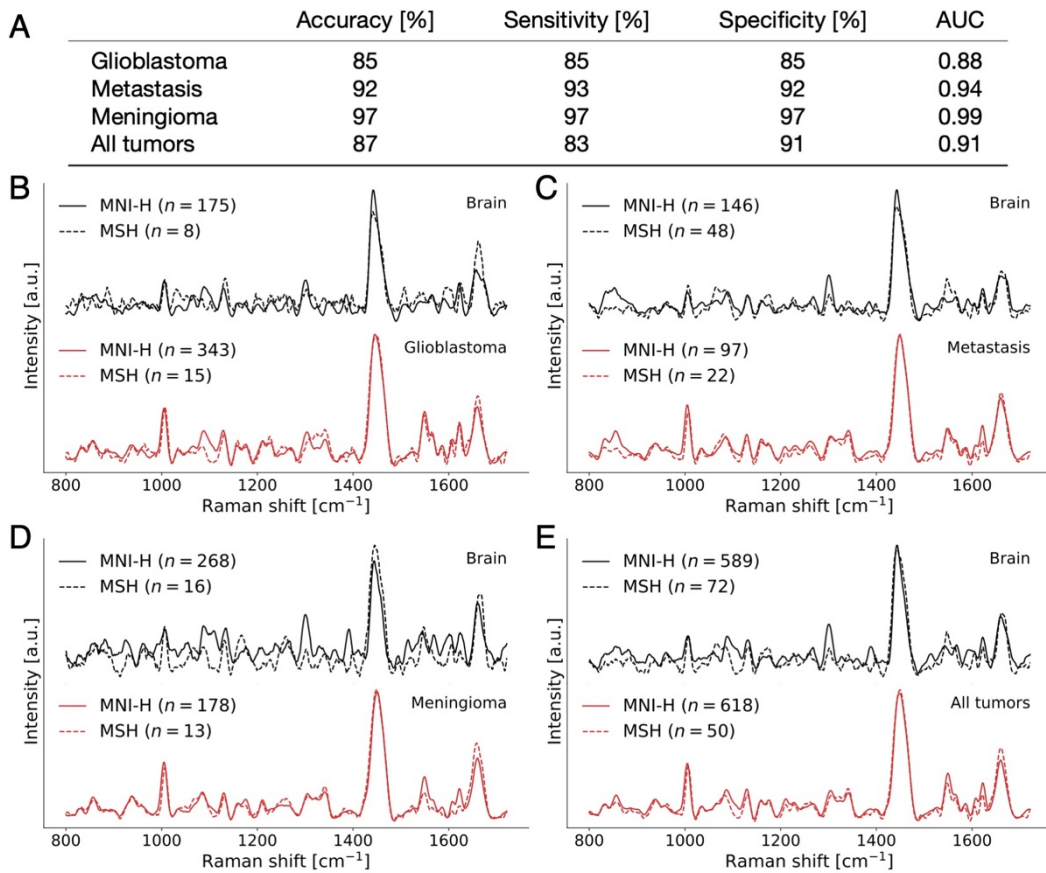


Figure S3. (A-D) Data from MNI-H and MSH showing spectral fingerprints from each medical center with quality factor applied. Spectral fingerprints were plotted for patients with (A) glioblastoma, (B) metastasis, (C) meningioma, and (D) all tumor types combined.



Supplementary Figure S4: (A-E) Machine learning model with no quality factor threshold applied to the data. (A) Table presenting all results from machine learning models discriminating between spectral fingerprints from non-tumoral brain and tumor in patients with different types of cancer. Spectral fingerprints were plotted for patients with (B) glioblastoma, (C) metastasis, (D) meningioma, and (E) all tumor types.